J Ther Eng, Vol. 7, No. 7, pp. 1752–1767, November, 2021

Journal of Thermal Engineering
Web page info: https://jten.yildiz.edu.tr
DOI: 10.14744/jten.2021.0006

Research Article

Numerical investigation of laminar forced convection and entropy generation of Fe_3O_4/water nanofluids in different cross-sectioned channel geometries

Edip TASKESEN[1,2,*], Mutlu TEKIR[3], Engin GEDIK[1], Kamil ARSLAN[4]

[1]*Department of Energy Systems Engineering, Faculty of Technology, Karabük University, Karabük, Turkey*
[2]*Department of Energy Systems Engineering, Faculty of Engineering, Şırnak University, Şırnak, Turkey*
[3]*Department of Medical Engineering, Faculty of Engineering, Karabük University, Karabük, Turkey*
[4]*Department of Mechanical Engineering, Faculty of Engineering, Karabük University, Karabük, Turkey*

ARTICLE INFO

Article history
Received: 22 June 2020
Accepted: 24 November 2020

Key words:
Nanofluid; Forced convection; Laminar flow; Cross-sectioned Channels

ABSTRACT

In this study, forced convection of nanofluid flow in various channel geometries with a hydraulic diameter of 16 mm and length of 1.5 m under laminar flow condition has been investigated numerically. Constant heat flux of 6 kW/m^2 has been applied on to the surfaces of the channels. Fe_3O_4/water nanofluid has been used in the analyses to enhance the convective heat transfer of the base fluid. Analyses have been performed for Reynolds numbers between 500≤Re≤2000, and for volume concentrations of nanoparticles between 1% and 5% in cylindrical, square, rectangle, and triangle cross-sectioned channel geometries. The finite volume discretization method has been used to solve the governing equations. The effects of some parameters; Reynolds number, nanoparticle volume fractions, channel geometries on the average Nusselt number, Darcy friction factor and entropy generation have been investigated in detail. The results indicate that nanofluid offers further convective heat transfer enhancement according to base fluid and cylindrical cross-sectioned channel gives the best heat transfer performance among other cross-sectioned channel geometries. Using water as a working fluid, cylindrical cross-sectioned channel geometry gives the highest heat transfer rate among other channel geometries, whereas triangle one gives the lowest. Cylindrical cross-sectioned channel geometry offers up to 77.6% enhancement compared to triangle cross-sectioned channel geometry for the same hydraulic diameter and same heat flux. However, triangle cross-sectioned channel geometry has highest convective heat transfer increment ratio (4.12%) for changing working fluid as water to nanofluid. Also, some new Nu correlations based on the channel geometries and nanoparticle volume fractions were proposed in the present study.

Cite this article as: Taskesen E, Tekir M, Gedik E, Arslan K. Numerical investigation of laminar forced convection and entropy generation of Fe_3O_4/water nanofluids in different cross-sectioned channel geometries. J Ther Eng 2021;7(7):1752–1767.

***Corresponding author.**
*E-mail address: ediptaskesen@karabuk.edu.tr

This paper was recommended for publication in revised form by Regional Editor Mohammad Rahimi-Gorji

Published by Yıldız Technical University Press, İstanbul, Turkey

INTRODUCTION

Higher heat transfer rates are targeted in modern industrial applications nowadays. Enhancement of the heat transfer characteristics of working fluids has become an important research topic. One of the enhancement methods is the utilization of nanofluids. Recently increasing interest in nanofluids has led to a significant improvement in heat transfer performance. Nanofluid is a suspension of very fine particles with dimensions less than 100 nm mixed with classical fluid (water, oil and ethylene glycol), which greatly improves the heat transfer characteristics of the base fluid [1]. Nanofluids are used in different fields such as refrigeration industry, nuclear reactors, drug transport system, automotive applications, fuels, microchips cooling and geothermal energy [2]. In recent years, experimental and numerical studies [3]–[4] on nanofluids have been carried out to further improve the heat transfer characteristics. Dalkılıc et al. [5] have reviewed the papers studies in this field to well understanding of the characteristics of nanofluids. Due to the fact that a good promising technology of the nanofluids in thermal engineering applications such kind of works with different geometries and flow conditions using nanofluids are increasing day by day. When these studies are examined, it can be seen that nanoparticle concentration is one of the most important parameters affecting heat transfer in such applications. Minea [6] studied the numerically to investigate the nanoparticle concentration effect on forced convection heat transfer in a tube. She used the single-phase model on the solution of Al_2O_3-water nanofluid flow for both laminar and turbulent regime. It is concluded that from the study heat transfer enhancement is increasing with the nanoparticle volume concentration. This conclusion has also been declared by Ekiciler et al. [7] for the laminar flow of SiO_2-water nanofluid flow in a duct. Ting et al. [8] investigated the convection heat transfer and flow characteristics of water-based Al_2O_3 nanofluids with different volumetric nanoparticle concentrations (0.1–2.0 vol.%) under the constant wall temperature boundary condition. In the laminar range ($360 \leq Re \leq 2100$) the heat transfer coefficient of the Al_2O_3/water nanofluid with 2 vol.% enhanced by 32% compared to the pure water. Heris et al. [9] studied Al_2O_3/water nanofluid flow experimentally through a square cross-sectioned channel under constant heat flux in laminar flow and observed up to 27.6% enhancement using 2.5 vol.% nanofluid comparing to the base fluid. Heris et al. [10] numerically analyzed laminar flow and heat transfer of three different nanofluids (Al_2O_3/water, CuO/water, and Cu/water) through a square cross-sectioned channel under constant heat flux conditions. Obtained enhancements of Nusselt number for Cu/water, CuO/water, and Al_2O_3/water nanofluids were 4.0% vol. 77%, 68% and 59% respectively. Yin et al. [11] studied Cu/water nanofluid flow both experimentally and numerically analyzing pressure drop and heat transfer in a pipe under laminar flow conditions. The results showed that the nanofluids below 2.5 vol.% increased heat transfer. Purohit et al. [12] investigated laminar flow of various nanofluids (Al_2O_3/water, ZrO_2/water, and TiO_2/water) in a circular tube. It was observed that 8-30% increment of heat transfer coefficient for all investigated nanofluids. Li et al. [13] investigated laminar convective heat transfer of Cu/water nanofluid having 0.5-2 vol.%. They reported that the heat transfer coefficient increases up to 60% for nanofluid with 2.0 vol.%. Wen et al. [14] investigated the heat transfer of α-Al_2O_3 nanofluid flow in a copper tube under the laminar flow conditions. They reported a 47% enhancement in local heat transfer coefficient at $x/D = 63$ and $Re=1600$ using nanofluid with 1.6 vol.%. Chen et al. [15] measured the effective thermal conductivity, rheological behavior and forced convective heat transfer of the nanofluids containing titanate nanotubes (0.5, 1.0, and 2.5 wt.%). They found that the titanate nanotube nanofluids with 2.5 wt.% showed a small thermal conductivity enhancement, i.e. ~3% at 25 ˚C and ~5% at 40 ˚C. Anoop et al. [16] experimentally investigated the convective heat transfer coefficient of alumina/water nanofluids. The authors reported that the heat transfer enhancement of the nanofluid with 4 wt.% containing 45 nm nanoparticles for $x/D=147$ at $Re=1550$ was around 25%, whereas for nanofluid containing 150 nm nanoparticles it was found to be around 11%. Davarnejad et al. [17] numerically investigated the heat transfer characteristics of Al_2O_3/water nanofluid in a circular tube under constant heat flux and showed that the convective heat transfer coefficient increases by increasing velocity and decreasing particle diameter. Abareshi et al. [18] prepared Fe_3O_4/water nanofluids. The results showed that the enhancement of the thermal conductivity increases 11.5% as the volumetric nanoparticle concentrations increases up to 3% at 40 ˚C. Turgut et al. [19] were studied the thermal conductivity of TiO_2/water with 3 vol.% at different temperatures (13 ˚C, 23 ˚C, 40 ˚C, and 55 ˚C). They found that up to 7.4% enhancement has been reached using TiO_2/water nanofluid with 3 vol.% at 13 ˚C. Fadhil et al. [20] used 3 vol.% SiO_2/water nanofluid in laminar flow conditions ($100 \leq Re \leq 1000$). As a result, they observed that the cooler base temperature decreased and the Nusselt number increased with increasing Reynolds number. Kaya et al. [21], have studied TiO_2/water nanofluid with different volumetric nanoparticle concentrations (ranging from 1.0 vol.%-4.0 vol.%) in a semi-circular cross-sectioned microchannel under steady-state laminar flow condition. As a result, an enhancement in the average Nusselt number can reach up to 10% along with increasing the volumetric nanoparticle concentration of TiO_2/water nanofluid.

Entropy generation due to the fluid friction and heat transfer is an important parameter to determine the heat transfer performance on various channels geometries as studied in this work. Uysal et al. [22] investigated the convective heat transfer and entropy generation of ZnO/EG nanofluid (1.0-4.0 vol.%) flow through square microchannel. As a result, it was found that when 4.0% ZnO

nanoparticles were added to pure EG at Re=100, the flow convective heat transfer coefficient increased from 9718.15 W/m^{2}K to 23010.79 W/m^{2}K. The total entropy production of the ZnO/EG nanofluid decreases with the increase in the volumetric nanoparticle concentration of the ZnO/EG nanofluid. In addition, that the convective heat transfer and entropy generation of diamond-Fe_3O_4/water hybrid nanofluid was numerically investigated by Uysal et al. [23]. In their study apart from the well-known conclusions they found minimum entropy generation rate for hybrid and conventional nanofluids. Li et al. [24] numerically investigated the entropy generation and forced convection heat transfer of Al_2O_3/water nanofluid in a heat exchanger equipped with a spiral band, the effect of height ratio and Reynolds number on entropy. As a result, they showed that the thermal entropy generation decreases with the height ratio and the increase of Re.

Even though investigations about nanofluids are plenty, and also notwithstanding the existence of literature dealing the convective heat transfer of various nanofluids, to the best of authors' knowledge, investigations about Fe_3O_4/water nanofluid are still limited and there is no comparative study available literature focusing on the effect of channel geometries. Motivated by this, the main objective of the present work is to investigate numerically forced convection heat transfer characteristics of Fe_3O_4/water nanofluid flow in different channel geometries (cylindrical, square, rectangular, triangular) having the same hydraulic diameters. For this purpose, some pertinent parameters such as channel geometries, volumetric nanoparticle concentrations effect on the convection heat transfer are examined under the laminar flow regime. In addition, that, in the study, the scope of the subject examined was expanded by considering entropy generation and new Nu number correlations are proposed. This study can provide a guidance for the usage of nanofluids flow in the engineering applications having various cross-sectioned channel geometries.

MATERIAL AND METHOD

Theoretical Background

In this study, flow and heat transfer characteristics of Fe_3O_4/water nanofluid flow in a channel with a hydraulic diameter of 16 mm and a length of 1.5 m were investigated numerically. The average convective heat transfer coefficient and Nusselt number are fundamental parameters to find out the thermal performance of the nanofluid that has been defined by the following equations [25];

$$h_{nf} = \frac{q''}{(T_w - T_b)_{avg}} \tag{1}$$

$$T_b = \frac{T_{in,nf} + T_{out,nf}}{2} \tag{2}$$

$$Nu_{nf} = \frac{h_{nf} \cdot D_h}{k_{nf}} \tag{3}$$

where $(T_w - T_b)_{avg}$ is the linear mean temperature difference of wall and the bulk temperature. The bulk temperature of the nanofluid flow can be determined from the taking average of the temperatures of the nanofluid at the inlet and the outlet sections of the channel, h is the average convective heat transfer, *Dh* is hydraulic diameter, *k* is the thermal conductivity, nf represent the nanofluid, *q″* is the heat flux.

Widely used correlations in literature are given below. Shah-London correlation [26] is expressed in Eq. 4, Gnielinski [27] correlation for laminar flow in Eq. 5, Churchill-Ozoe correlation [28] in Eq. 6, and Sieder-Tate [29] correlation for laminar flow in Eq. 7.

$$Nu = 1.953 \cdot \left(\mathrm{Re} \cdot \mathrm{Pr} \cdot \frac{D}{L} \right)^{1/3} ; \quad \left(\mathrm{Re} \cdot \mathrm{Pr} \cdot \frac{D}{L} \right) \geq 33{,}3 \tag{4}$$

$$\begin{aligned} Nu = \Big[& 4.354^3 + 0.6^3 \\ & + (1.953 \sqrt[3]{\mathrm{Re} \cdot \mathrm{Pr} \cdot D/L} - 0.6)^3 \\ & + (0.924 \sqrt[3]{\mathrm{Pr}} \sqrt{\mathrm{Re} \cdot D/L})^3 \Big]^{1/3} \end{aligned} \tag{5}$$

$$\begin{aligned} Nu = 4.364 & \left[1 + \left(\frac{\pi}{4} \frac{\mathrm{Re} \cdot \mathrm{Pr}}{L/D} \Big/ 29.6 \right)^2 \right]^{1/6} \\ & \times \left[1 + \left(\frac{\frac{\pi}{4} \frac{\mathrm{Re} \cdot \mathrm{Pr}}{L/D} \Big/ 19.04}{\left[1 + \left(\mathrm{Pr} / 0.0207 \right)^{2/3} \right]^{1/2} \left[1 + \left(\frac{\pi}{4} \frac{\mathrm{Re} \cdot \mathrm{Pr}}{L/D} \Big/ 29.6 \right)^2 \right]^{1/3}} \right)^{3/2} \right] \end{aligned} \tag{6}$$

$$Nu = 1.86 \mathrm{Re}^{1/3} \mathrm{Pr}^{1/3} \left(\frac{D}{L} \right)^{1/3} \tag{7}$$

f is the average Darcy friction factor that is found from the Darcy-Weisbach equation given below [25]:

$$f = \frac{\Delta P}{\left(\frac{L}{D_h} \right) \times \left(\frac{\rho \times V^2}{2} \right)} \tag{8}$$

Numerical analyses can be made with three different approaches: i) Single Phase Model, ii) Euler-Euler Approach and Euler-Lagrange Approach. In this study Single Phase Model was used. Physical properties of the nanofluids are calculated from water and nanoparticle characteristics

at the mean temperature using the following equations [30–32]:

$$\rho_{nf} = (1-\varphi)\rho_{bf} + \varphi\rho_{np} \tag{9}$$

$$(\rho C_p)_{nf} = (1-\varphi)(\rho C_p)_{bf} + \varphi(\rho C_p)np \tag{10}$$

$$\frac{k_{nf}}{k_f} = \frac{k_{np} + 2k_{bf} - 2\varphi(k_{bf} - k_{np})}{k_{np} + 2k_{bf} + \varphi(k_{bf} - k_{np})} \tag{11}$$

$$\mu_{nf} = \frac{\mu_{bf}}{(1-\varphi)^{2.5}} \tag{12}$$

where bf, np and nf represents the base fluid, nanoparticle and nanofluid respectively whereas ρ, φ, C_p and μ denotes density, nanoparticle volume concentration, thermal capacity and dynamic viscosity.

The thermophysical properties of pure water, Fe_3O_4 and nanofluids are given in Table 1 at the bulk temperature which were obtained from the study of Dibaei and Kargarsharifabad [33].

Reynolds and Prandtl numbers are calculated from the equations below [25]:

$$\mathrm{Re}_D = \frac{\rho_{nf} V D_h}{\mu_{nf}} \tag{13}$$

$$\mathrm{Pr}_{nf} = \frac{C_{pnf}\mu_{nf}}{k_{nf}} \tag{14}$$

Performance evaluation criteria is the ratio to consider the effects of heat transfer enhancement and additional pumping power as a result of using nanofluid instead of base fluid. Greater the PEC ratio means greater heat transfer performance despite the pressure drop increase. Also, the PEC ratio describes the efficiency of the nanofluid used in the system, and it is defined below [32]. Likewise, efficiency increases with increasing both the Reynolds number and volume concentration.

$$PEC = \frac{\left(Nu_{enhanced} / Nu_{base}\right)}{\left(f_{enhanced} / f_{base}\right)^{1/3}} \tag{15}$$

Entropy can be characterized as an extensive property that becomes somewhat more meaningful when the microscopic state of the system and its surroundings is considered. Although physically defining of entropy concept is difficult, it can be clarified as a measure of molecular disorder, or molecular randomness which means that the positions of the molecules become less predictable and the entropy increases in case a system becomes more disordered. Thus, the entropy change of the system during an irreversible process is directly associated with increasing of molecular chaos of a substance or a fluid flow. From a more fundamental point of view, the second law of thermodynamics gives us a clear picture of where entropy is generated from. Accordingly, the total entropy generation rate per the length of the channel due to heat transfer (with finite temperature difference) and flow friction during through non-circular channel is expressed as follows:

$$\dot{S}'_{gen} = \dot{S}'_{gen,\ heat\ transfer} + \dot{S}'_{gen,\ fluid\ friction} \tag{16}$$

For simplicity, if a small passage of length dx is considered as the thermodynamic system, the first law of thermodynamics can be written as [34]:

$$\dot{m}dh = q'dx \tag{17}$$

Hence, the correlation above becomes:

$$\dot{S}'_{gen} = \frac{\dot{m}ds}{dx} - \frac{q'}{T + \Delta T} \tag{18}$$

where T denotes the fluid bulk temperature. For an incompressible fluid, the Gibbs equation [35] can be given as:

$$Tds = dh - \upsilon dP \tag{19}$$

where υ denotes the specific volume expressed as:

$$\upsilon = \frac{1}{\rho} \tag{20}$$

If the expressions between Eqs. (18) and (20) are combined, the entropy generation rate, $\dot{S}'_{gen}$ is obtained as follows:

$$\dot{S}'_{gen} = \frac{q'\Delta T}{T^2 + T\Delta T} + \frac{\dot{m}}{T\rho}\left(-\frac{dP}{dx}\right) \tag{21}$$

Table 1. Thermophysical properties of water, Fe_3O_4 nanoparticles, Fe_3O_4/water nanofluids at various volumetric nanoparticle concentrations [33]

The properties of the working fluid	Water	Fe_3O_4	1 vol.% Fe_3O_4/water	2 vol.% Fe_3O_4/water	5 vol.% Fe_3O_4/water
Density (kg/m^3)	998	5180	1041	1083	1209
Thermal conductivity (W/mK)	0.6	80.4	0.6096	0.6186	0.665
Specific Heat (J/kgK)	4182	670	4152	4122	4022
Viscosity (kg/ms)	1.003	–	1.0806	1.16	1.3

In Eq. (23), the differential form of pressure drop across the system, P can be derived as given:

$$P(x) = f\frac{x}{D_h}\frac{\rho V^2}{2} \tag{22}$$

$$-\frac{dP}{dx} = f\frac{\rho V^2}{2D_h} = f\frac{\rho V^2 P_c}{8A_c} \tag{23}$$

Since the mass flow rate, ṁ is defined as:

$$\dot{m} = \rho V A_c \tag{24}$$

Using this relation, the above equation can be simplified as:

$$-\frac{dP}{dx} = \frac{\dot{m}^2 \cdot f \cdot P_c}{8\rho A_c^3} \tag{25}$$

If ΔT is left alone on the left hand side in Eqs. (2) and (3), it is determined as:

$$\Delta T = \frac{q'}{h \cdot P_c} = \frac{q'}{\frac{Nu \cdot k}{D_h} \cdot P_c} = \frac{q'}{Nu \cdot k \cdot \frac{P_c^2}{4A_c}} = \frac{4q' \cdot A_c}{Nu \cdot k \cdot P_c^2} \tag{26}$$

Finally, a generalized entropy generation rate for a non-circular cross-sectioned channel is obtained by using Eqs. (21), (25) and (26):

$$\dot{S}'_{gen} = \frac{\frac{4(q')^2 \cdot A_c}{Nu \cdot k \cdot P_c^2}}{T^2 + \frac{T \cdot 4q' \cdot A_c}{Nu \cdot k \cdot P_c^2}} + \frac{\dot{m}}{T\rho}\left(\frac{\dot{m}^2 \cdot f \cdot P_c}{8\rho A_c^3}\right) \tag{27}$$

$$\dot{S}'_{gen} = \frac{4(q')^2 \cdot A_c}{T^2 Nu \cdot k \cdot P_c^2 + 4T \cdot q' \cdot A_c} + \frac{f \cdot \rho V^3 \cdot P_c}{8T} \tag{28}$$

NUMERICAL PROCEDURE

Numerical analysis is performed to compare the heat transfer characteristics of the nanofluid flow in different cross-sectioned channels having same hydraulic diameter. Schematic illustration of the channel geometries is given in Figure 1. The diameter and length of the cylindrical cross-sectioned channel are 1.6 cm and 1.5 m, respectively. The edges of the square cross-sectioned channel geometry are 1.6 cm. Dimensions of the rectangle cross-sectioned channel geometry are 1.3 cm × 2.1 cm x 1.5 m. The edges of the triangle cross-sectioned channel geometry are equilateral, and 2.77 cm.

The nanofluid is incompressible, and the flow is assumed to be steady-state and laminar. The inlet temperature of the fluid is assumed constant (300 K). The constant heat flux (6 kW/m²) is applied on the outer walls of the channel geometries. The velocity inlet, zero pressure outlet and no-slip wall boundary condition were applied in the numerical computations. The thermophysical properties of the nanofluid are constant. The nanofluid is assumed to be single phase (homogeneous) model. In this model, the nanofluid is treated as a homogeneous fluid with effective properties because of nanoparticle addition since the mixture acts as a single-phase fluid. Apart from this model, Euler-Euler and Euler-Lagrange approaches are also employed in some studies for two phase analysis in the literature. All models have advantages and disadvantages. However, single phase model comes to the forefront among these since other models does not provide an insight into complicated numerical models [36]. In the laminar regime,

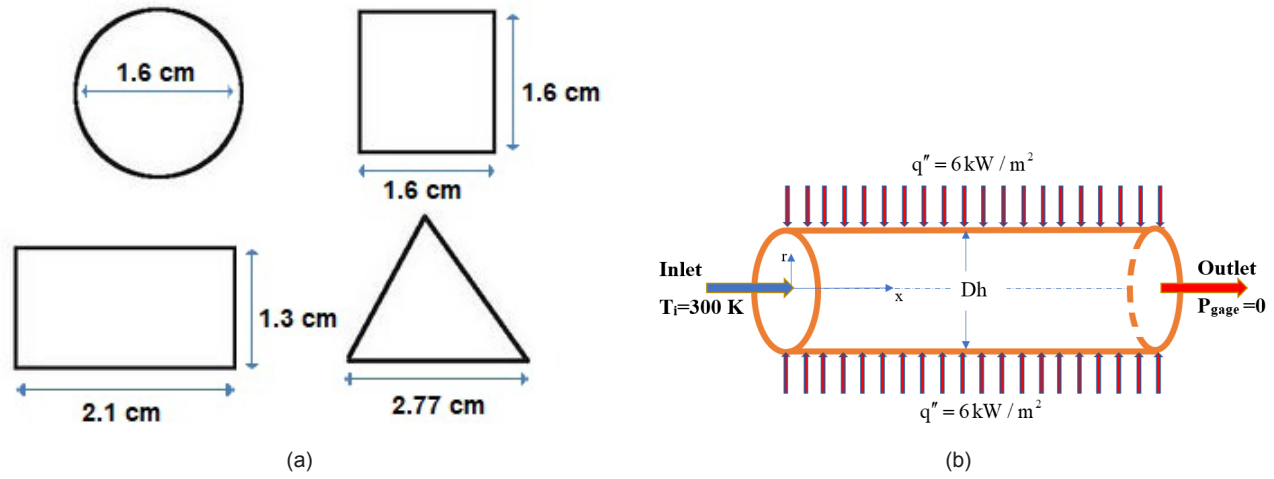

Figure 1. (a) Different cross-sectioned channel geometries with same hydraulic diameters and (b) boundary condition of the problem for cylindrical channel.

different Reynolds numbers ranging from 500 to 2000 are taken into consideration. Besides, the Reynolds number is determined as functions of average velocity of the nanofluid, the hydraulic diameter of the channels and the thermophysical properties of nanofluids.

In the numerical analysis, commercial CFD software Ansys Fluent 19.1 was used. This software uses the finite-volume method to perform the numerical calculations by solving governing equations (29-31) along with the boundary conditions. For incompressible, constant thermophysical properties and negligible dissipation; continuity, momentum, and energy equations are given below, respectively [37]:

$$\nabla \cdot \vec{V} = 0 \tag{29}$$

$$\rho \frac{D\vec{V}}{Dt} = \rho \vec{g} - \nabla p + \mu \nabla^2 \vec{V} \tag{30}$$

$$\rho C_p \frac{DT}{Dt} = k \nabla^2 T \tag{31}$$

The convection terms in continuity, momentum, and energy were discretized using the second-order upwind scheme. For the discretization of pressure, the standard scheme was used and for pressure-velocity coupling, the SIMPLE algorithm was utilized. The least-square cell-based method was applied for the discretization of the equations. For convergence, iterations were continued until the residuals fall below 10^{-6}. As shown in Figure 2, the hexahedral mesh was used for the cylindrical, square, rectangular, and triangle cross-sectioned channels, and mesh intensity was increased near the wall to enhance the accuracy and to simulate better thermal characteristics in the boundary layer.

The essential factor that affects the accuracy of results is quality and cell number of mesh. Poor quality mesh or smaller mesh number causes to decrease the accuracy of results, while a higher mesh number increases computational time. Therefore, grid independence test is very crucial to reach reasonable accuracy of results within reasonable computational time. Grid independence studies have been performed for all cross-sectioned channels to obtain this balance. As can be seen in Figure 3 and Table 2 below, optimum mesh numbers have been determined for different cross-sectioned channels. It can notice from Table 2, 140000, 515000, 700000 and 700000 cell number has been used for cylindrical, square, rectangle, and triangle cross-sectioned channel geometries, respectively.

RESULTS AND DISCUSSION

Results of cylindrical cross-sectioned channels using distilled water are compatible with the well-known correlations widely used in literature and is shown in Figure 4. Numerical results are in good agreement with the Sieder-Tate [29] correlation within +5% error margin, with the Gnielinski [27] correlation within +7% error margin, while with the Shah-London [26] correlation within +10% error margin.

On the other hand, experimental results are limited in the research area of non-circular cross-sectioned channels. However, Heris et al. [9] experimentally investigated nanofluid flow in a square cross-sectioned channel under laminar flow conditions. Hence, numerical results of this investigation have been compared with the experimental data of Heris et al. [9]. Results of the rectangle and square cross-sectioned channels are in good agreement within +10% error margin, while numerical results are within +5% error margin compared to the results of Churchill-Ozoe [28]. On the other hand, triangle cross-sectioned channel offers lower heat transfer compared to other non-circular cross-sectioned channels as can be seen in Figure 5. Furthermore, the friction factor of the cylindrical cross-sectioned channel using distilled water is higher than the non-circular cross-sectioned channels. For further verification of the mesh, the friction factor of the cylindrical cross-sectioned channel was compared with the Morrison model [38] in Figure 6, and it is within 8% error margin.

Laminar flow of Fe_3O_4/water nanofluid flow in different channel geometries having D_h=16 mm was investigated numerically to observe convective heat transfer characteristics and obtained results depicted graphically for a detailed discussion. Figure 7 shows the Nu number variations with Re number.

It can be seen that from the figure higher volumetric nanoparticle concentration nanofluid increases the convective heat transfer compared to distilled water. Also,

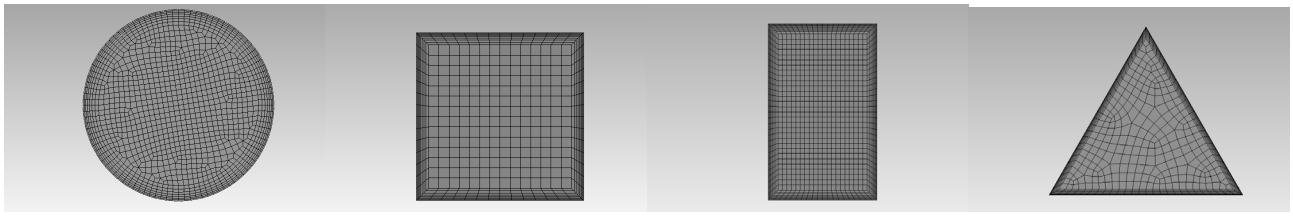

Figure 2. Mesh distribution of (a) cylindrical, (b) square, (c) rectangular, and (d) triangle cross-sectioned channels.

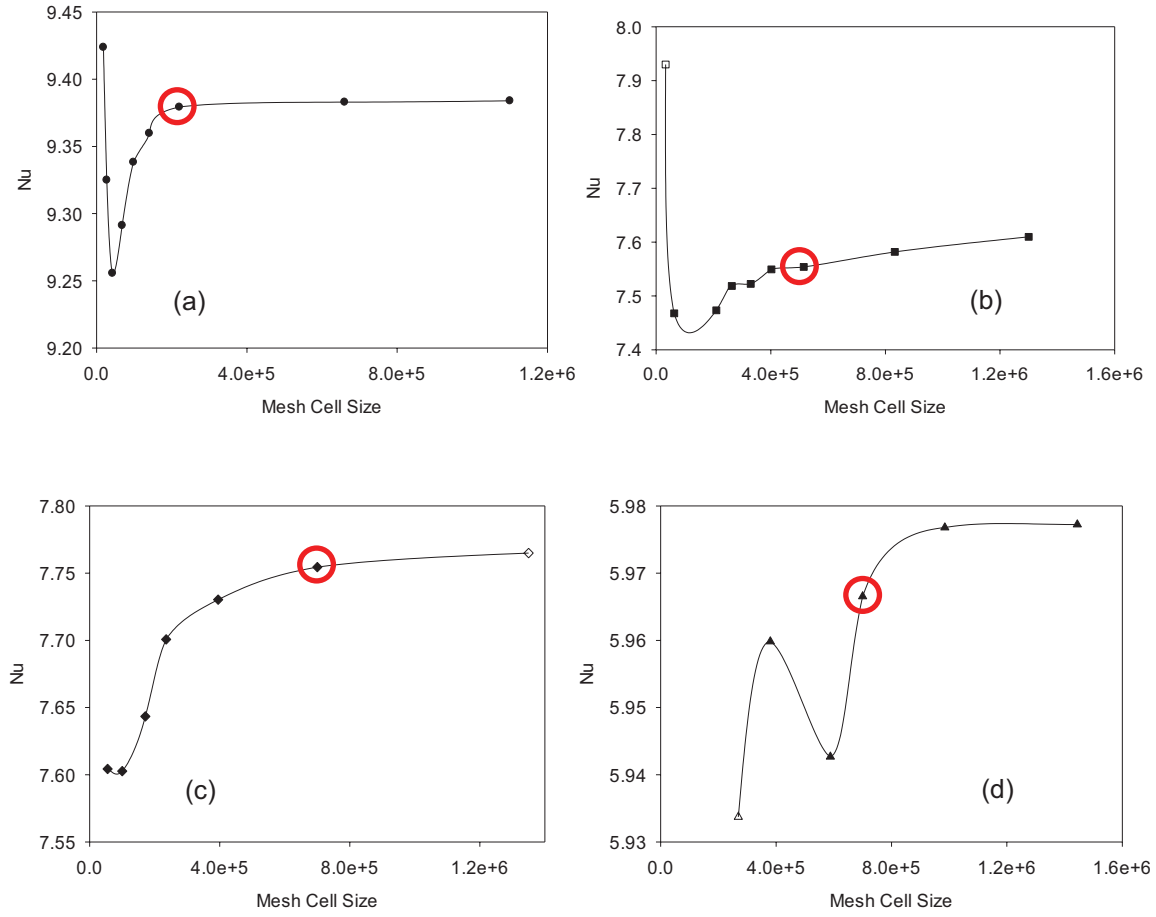

Figure 3. Grid independence test for (a) cylindrical, (b) square, (c) rectangular, and (d) triangle cross-sectioned channel geometries.

increasing Reynolds number increases the heat transfer performance of the working fluid. As can be seen in Figure 8, increasing volumetric nanoparticle concentration does not affect the Nusselt number significantly for the same Reynolds numbers and cross-section channels. On the other hand, the cross-sectioned channel type plays an essential role in heat transfer performance. It is proved to be cylindrical cross-sectioned channel is the best option, while the triangle cross-sectioned channel is the worst for heat transfer applications. Cylindrical cross-sectioned channel geometry offers up to 77.6% convective heat transfer enhancement compared to triangle cross-sectioned channel geometry. Square cross-sectioned channel geometry up to 36.4%, and rectangular cross-sectioned channel geometry up to 40.1% enhancement compared to triangle cross-sectioned channel geometry for the same hydraulic diameter and same heat flux. Triangle cross-sectioned channel geometry shows worst heat transfer performance among all.

In cylindrical cross-sectioned channel geometry; 1 vol.% Fe_3O_4 offers 1.59%, 2 vol.% Fe_3O_4 3.14%, and 5 vol.% Fe_3O_4 3.67% increase compared to distilled water. In rectangular cross-sectioned channel geometry; 1 vol.% Fe_3O_4 offers 1.59%, 2 vol.% Fe_3O_4 3.11%, and 5 vol.% Fe_3O_4 3.64% increase compared to distilled water. In square cross-sectioned channel geometry; 1 vol.% Fe_3O_4 offers 1.68%, 2 vol.% Fe_3O_4 3.33% and 5 vol.% Fe_3O_4 increased 3.9% increase compared to distilled water. In the triangle cross-sectioned channel geometry; 1 vol.% Fe_3O_4 offers 1.78%, 2 vol.% Fe_3O_4 3.52% and 5 vol.% Fe_3O_4 4.12% increase compared to distilled water. The best increase using nanofluid as working fluid compared to distilled water is achieved in triangular geometry. Cylindrical cross-sectioned channel geometry offers up to 77.6% enhancement, square cross-sectioned channel geometry up to 36.4%, and rectangular cross-sectioned channel geometry up to 40.1% enhancement compared to triangle cross-sectioned channel geometry for the same hydraulic diameter and same heat flux.

Nusselt number increase of triangle cross-sectioned channel compared to friction factor increase is much more than other cross-sectioned channels, so triangle cross-sectioned channel is more efficient than others. Also, the cylindrical cross-sectioned channel is seen to be the least efficient, while efficiencies of square and rectangle cross-sectioned channels are on average. 5% Fe_3O_4/water nanofluid has

Table 2. Numerical results of grid independence tests for all cross-sectioned channel geometries considered in the study

Cylindrical				Square			
Case	**Mesh No (x1000)**	**Nu**	**Change**	**Case**	**Mesh No (x1000)**	**Nu**	**Change**
1	18	9.424	-	1	33	7.930	–
2	27	9.325	–1.05%	2	63	7.468	–5.83%
3	42	9.256	–0.74%	3	210	7.473	0.07%
4	68	9.291	0.38%	4	264	7.519	0.61%
5	98	9.338	0.51%	5	330	7.522	0.05%
6	140	9.360	0.23%	6	402	7.549	0.36%
7	220	9.379	0.21%	7	515	7.554	0.06%
8	1100	9.384	0.05%	8	833	7.582	0.37%
				9	1300	7.610	0.37%
Rectangle				**Triangle**			
Case	**Mesh No (x1000)**	**Nu**	**Change**	**Case**	**Mesh No (x1000)**	**Nu**	**% Change**
1	55	7.604	–	1	369	5.934	–
2	100	7.603	–0.02%	2	408	5.960	0.44%
3	171	7.643	0.54%	3	588	5.943	–0.29%
4	235	7.701	0.75%	4	700	5.967	0.40%
5	395	7.730	0.38%	5	985	5.977	0.17%
6	700	7.755	0.31%	6	1570	5.979	0.04%
7	1535	7.777	0.29%				

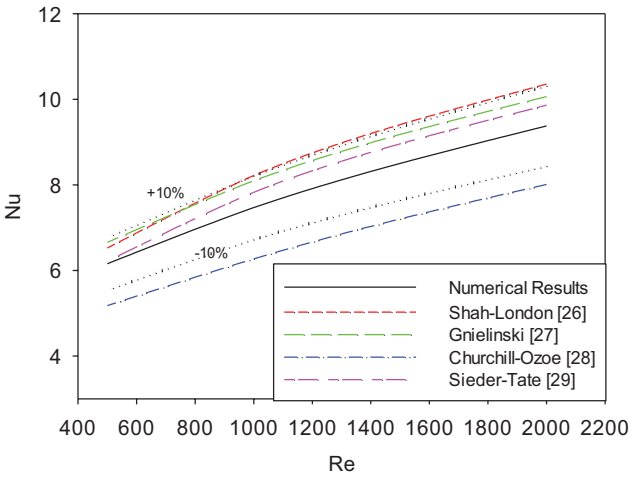

Figure 4. Comparison of numerical results using the cylindrical cross-sectioned channel with well-known correlations in the literature.

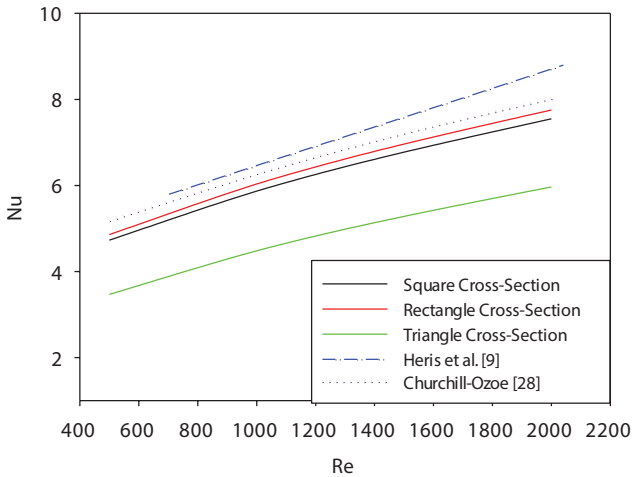

Figure 5. Comparison of numerical results using non-circular cross-sectioned channels with the results in the literature.

higher efficiency than the others. Even though the sharp edges of non-circular channels cause accumulation of heat and higher temperatures at these edges, decreases Nusselt numbers; non-circular cross-sectioned channels have lower friction factors than cylindrical cross-sectioned channel as can be seen in Figure 9–10. However, increasing volumetric nanoparticle concentration does not change the friction factor slightly even though the viscosity increase. On the contrary, even though triangle cross-sectioned channel is the worst for heat transfer rate among others, performance evaluation criteria (PEC) of triangle cross-sectioned channel is the best according to Figure 11.

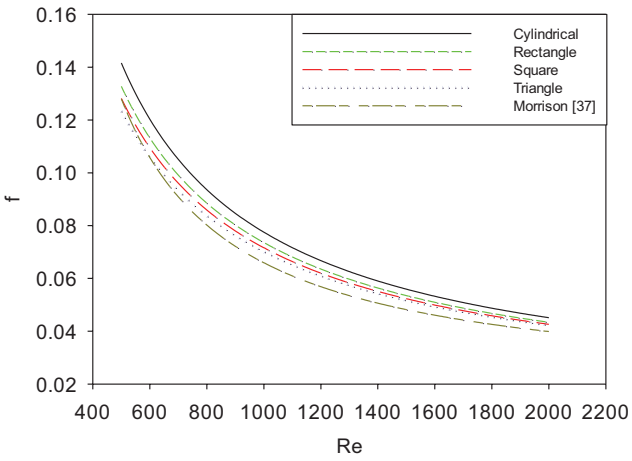

Figure 6. Comparison of friction factors of different cross-sectioned channels.

As can be seen in Figure 12, water has the highest entropy generation rate because it has lower heat transfer performance than the nanofluids. According to the results, 5 vol.% nanofluid has the lowest entropy generation rate. In Figure 13, triangle cross-sectioned channel geometry has the highest entropy generation rate, because heat accumulates in the edges and this increases entropy of the system, hence decreases the efficiency. Whereas cylindrical cross-sectioned channel has the lowest entropy generation rate, because heat spreads evenly on the wall cross-section. Square and rectangular cross-sectioned channel geometries have similar performances. Yet, square cross-sectioned channel geometry is better than rectangular one.

Lower Reynolds numbers has higher entropy generation rate than higher Reynolds numbers. This is related with the wall temperature. 5 vol.% nanofluid offers 12.1% lower entropy generation rate, while 2 vol.% offers 5.5% lower, 1 vol.% offers 2.9% lower entropy generation compared to

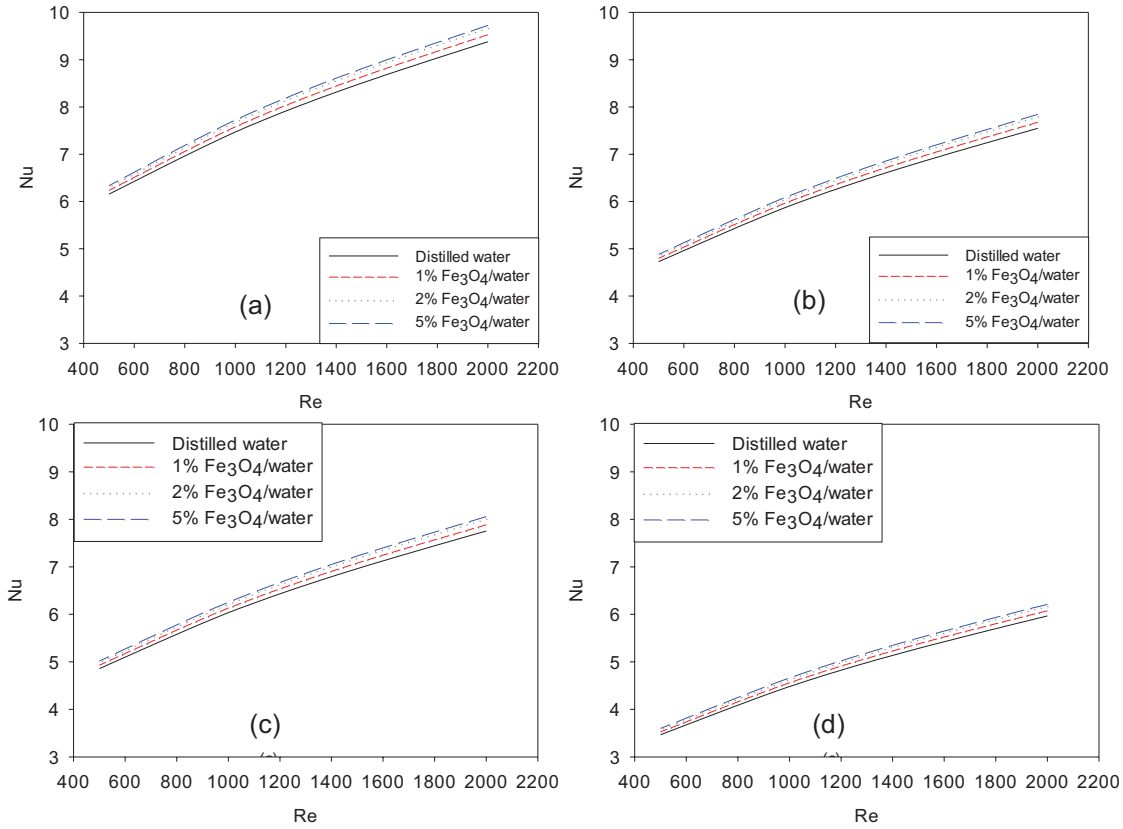

Figure 7. Nu number variations of Fe_3O_4/water nanofluid flow in (a) cylindrical, (b) square, (c) rectangular, and (d) triangle cross-sectioned channel geometries.

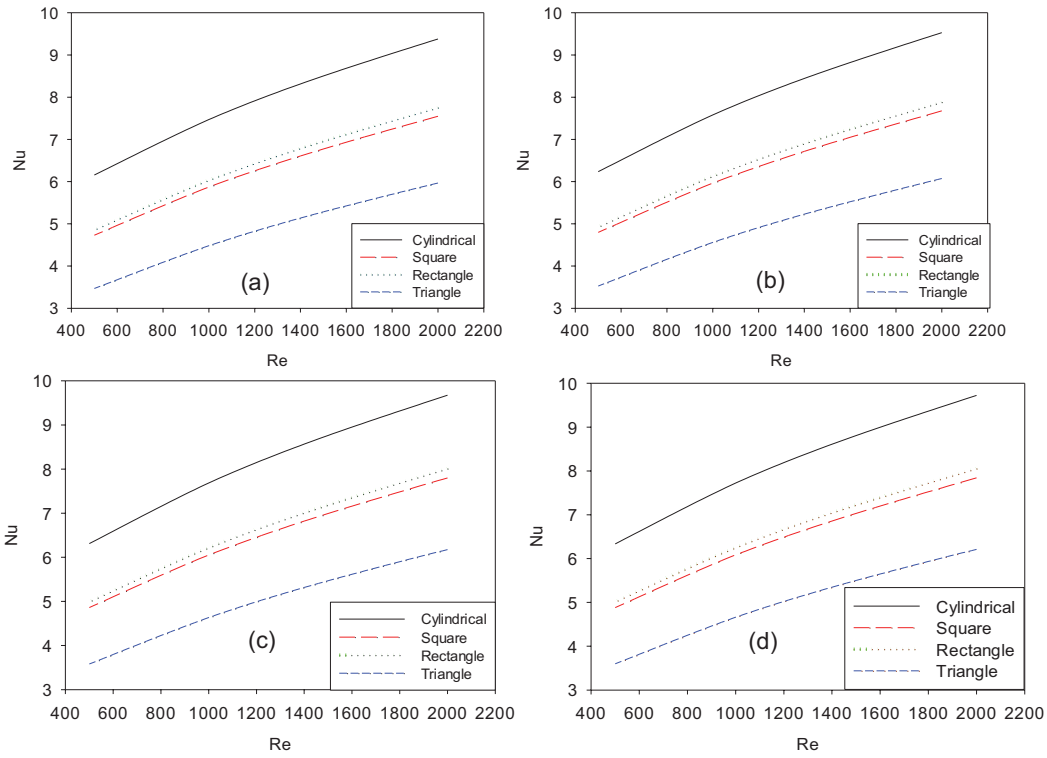

Figure 8. Nu number comparison of cross-sectioned channel geometries using (a) distilled water, (b) 1% Fe_3O_4/water, (c) 2% Fe_3O_4/water, and (d) 5% Fe_3O_4/water nanofluids.

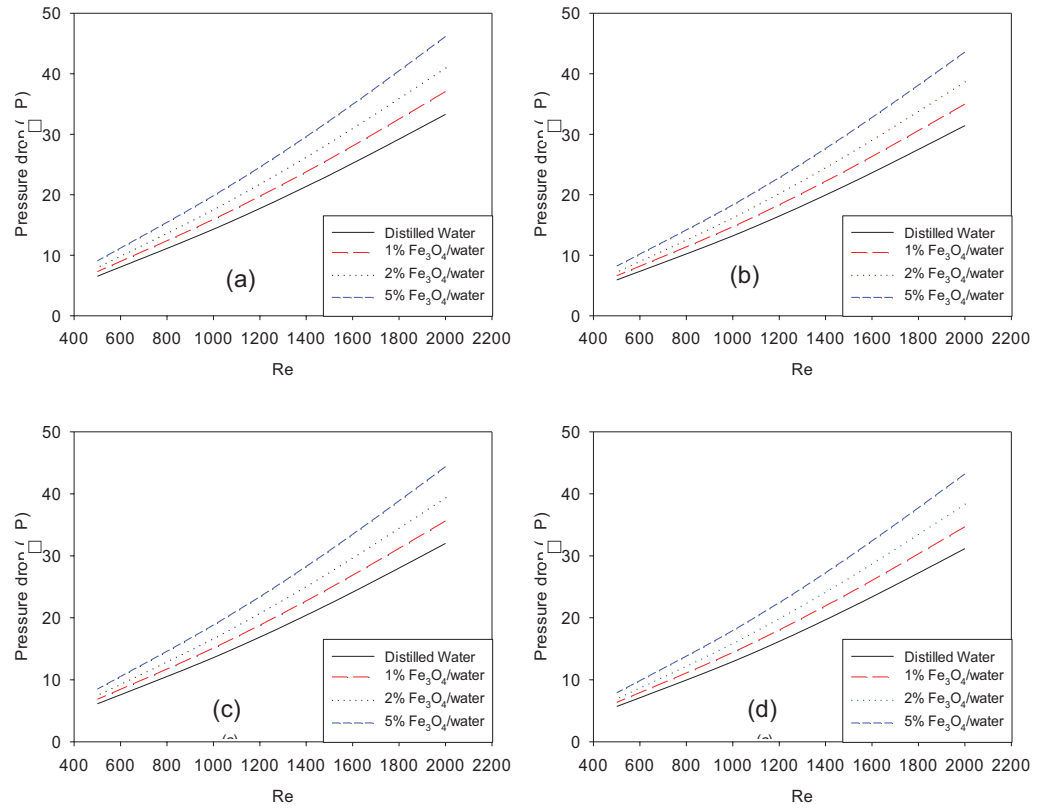

Figure 9. Pressure drop variations of Fe_3O_4/water nanofluid flow in (a) cylindrical, (b) square, (c) rectangular, and (d) triangle cross-sectioned channels.

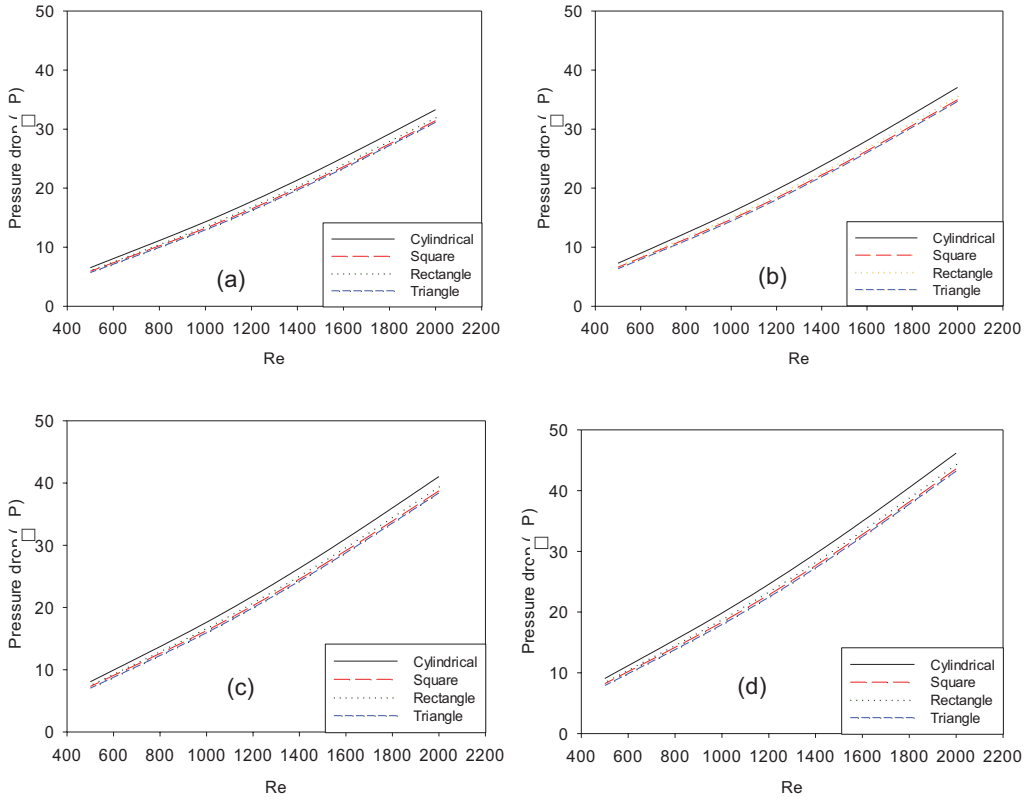

Figure 10. Pressure drop comparison of cross-sectioned channels using (a) distilled water, (b) 1% Fe_3O_4/water, (c) 2% Fe_3O_4/water, and (d) 5% Fe_3O_4/water nanofluids.

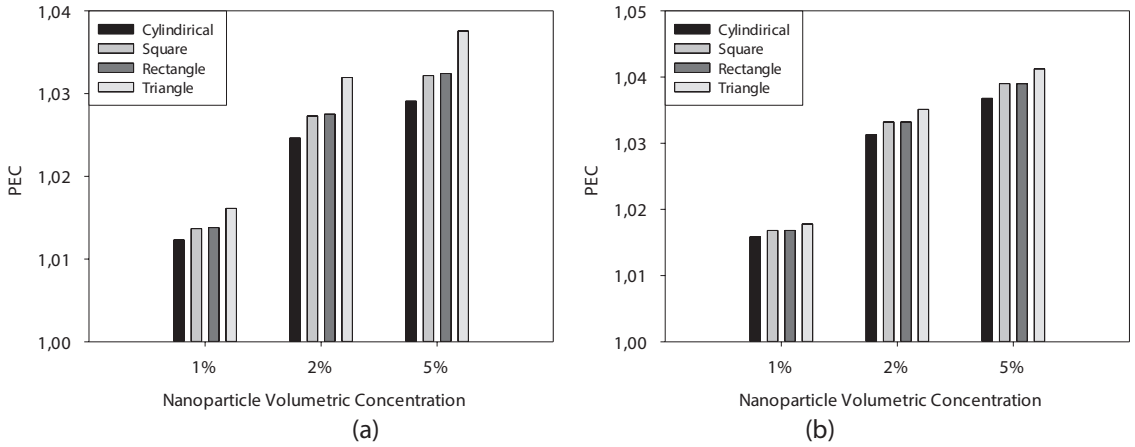

Figure 11. Performance evaluation criteria of nanofluids at various volume concentrations for different cross-sectioned channels at (a) Re=500 and (b) Re=2000.

water. Triangle cross-sectioned channel geometry has up to 63.7% entropy generation, rectangular cross-sectioned channel geometry has up to 40.6%, square cross-sectioned channel geometry has up to 38.2% more entropy generation rate than cylindrical cross-sectioned channel geometry. Also, higher entropy generation occurs from the heat transfer process, because fluid friction is so low due to laminar flow conditions. Consequently, even though PEC of triangle cross-sectioned channel geometry is the highest, this does not mean that its efficiency is highest. PEC shows that using nanofluid on triangle cross-sectioned channel geometry further increases Nusselt number, compared to the other channel geometries. However, it has the highest entropy generation rate, so lowest efficiency.

Pressure, velocity and temperature contours of cylindrical, square, rectangular, and triangle cross-sectioned channels at x=0m, x=0.5m, x=1.0m, and x=1.5m from the inlet are given in Figure 14. Thermally developing flow can be

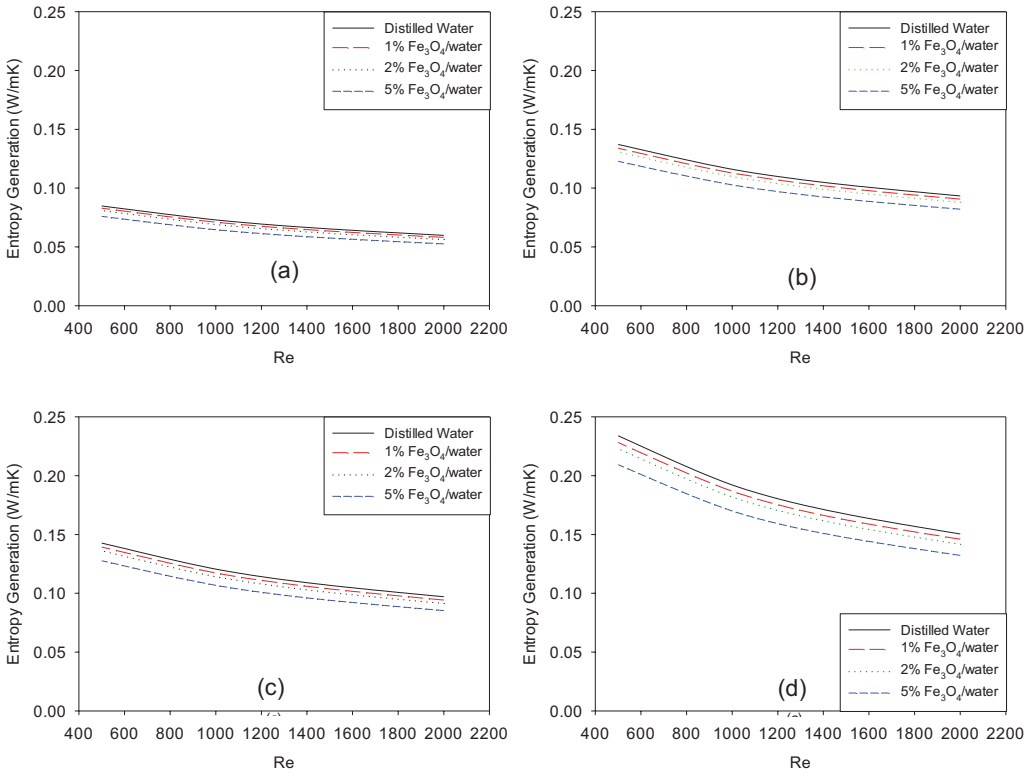

Figure 12. Entropy generation variations of Fe_3O_4/water nanofluid flow in (a) cylindrical, (b) square, (c) rectangular, and (d) triangle cross-sectioned channels.

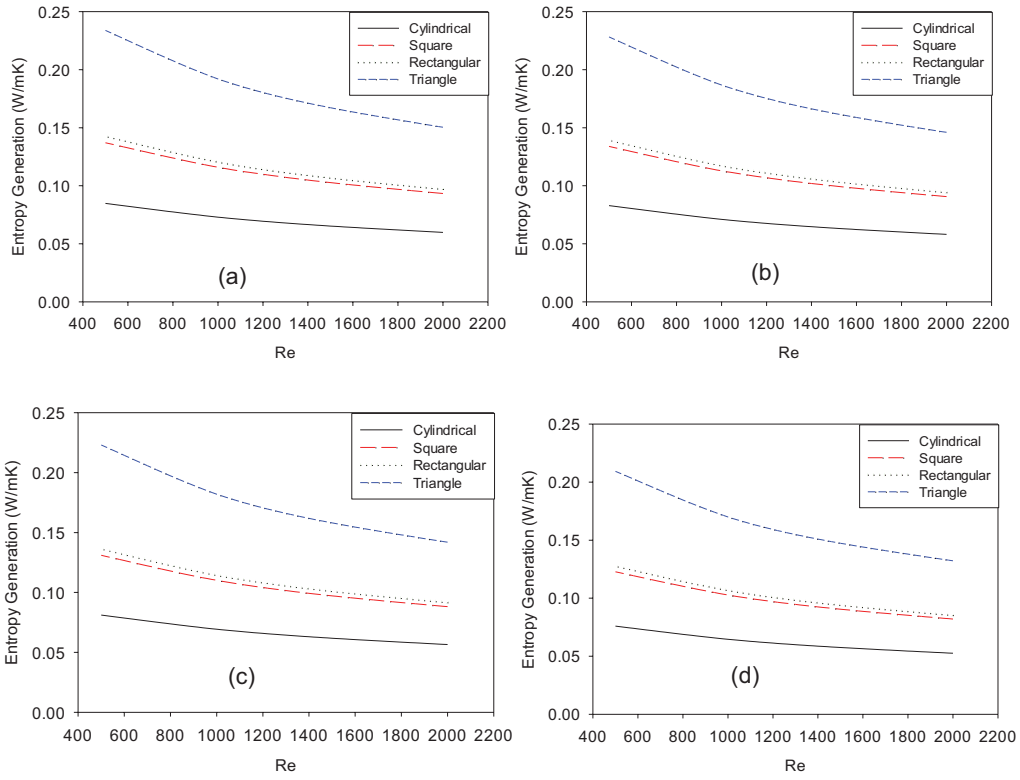

Figure 13. Entropy generation comparison of cross-sectioned channels using (a) distilled water, (b) 1% Fe_3O_4/water, (c) 2% Fe_3O_4/water, and (d) 5 vol.% Fe_3O_4/water nanofluids.

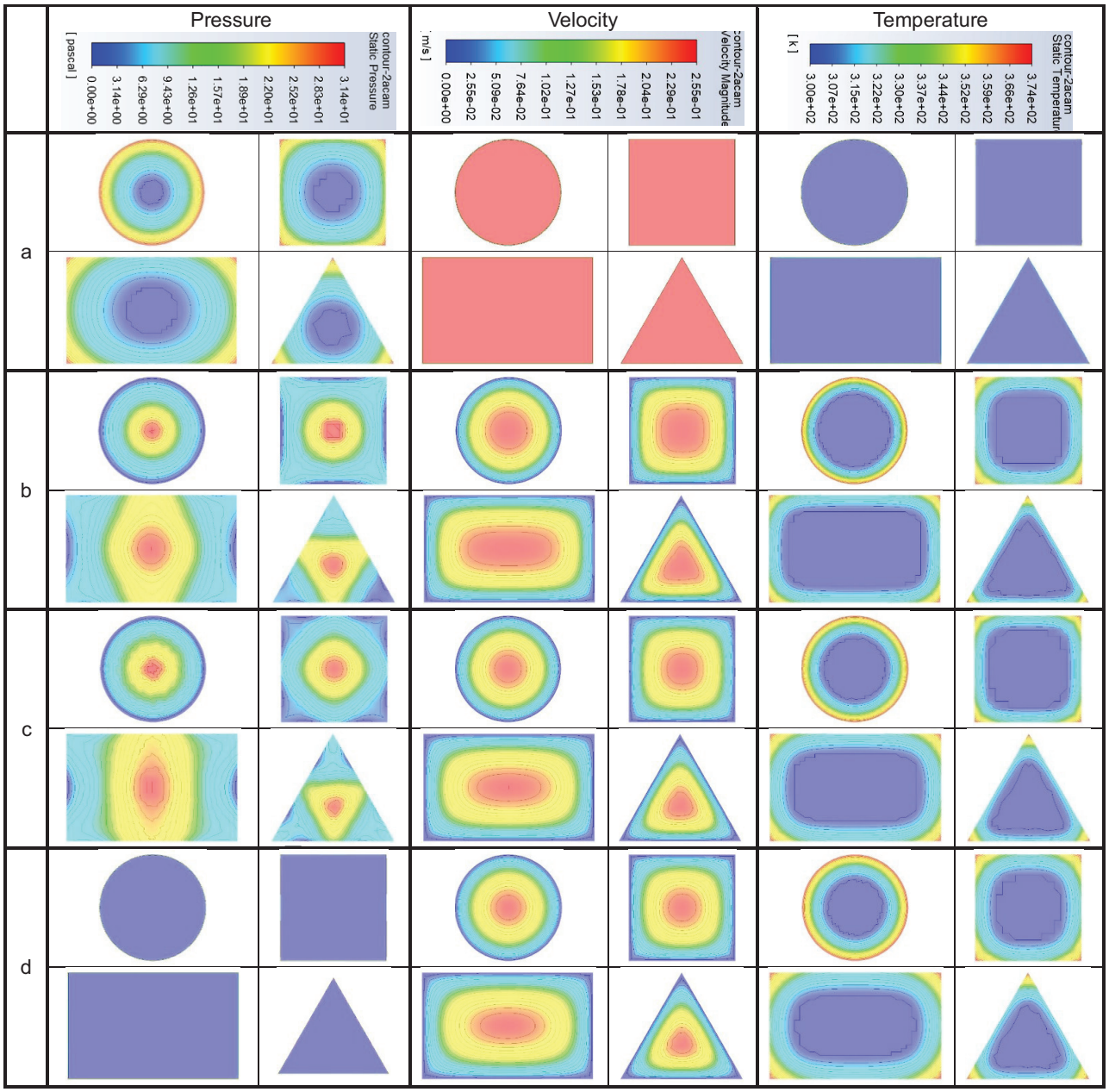

Figure 14. Contours graph of pressure, velocity and temperature distributions for different channel geometries at (a) x=0m, (b) x=0.5m, (c) x=1.0m, (d) x=1.5m.

seen in temperature contours, whereas hydrodynamically developing flow can be seen in velocity contours as contours proceed from inlet to outlet sections. It is clear that the flow near edges slow down as a result of no-slip condition, and higher temperature gradient develops near edges. This phenomenon causes Nusselt number to decrease. For the same flow conditions, the highest temperature is reached with triangle cross-sectioned channel geometry, and the lowest one is with cylindrical cross-sectioned channel geometry. As can be seen from Figure 14, it is clear that cylindrical channel geometry has minimum entropy generation, whereas non-circular channel geometries have maximum entropy generation in triangular geometry due to higher wall temperatures at their edges.

After a detailed discussion of the results, as can be seen in Equation 32, a new Nu correlation equation based on the Re number, the volumetric nanoparticle concentration and some constants has been proposed. It has also been developed for cylindrical, square, rectangle, and triangle cross-sectioned channel geometries and constants are given

Table 3. Constants of channel geometries for the correlation

Channels / Constants	a	b	c
Cylindrical	0.873747	0.312881	4.98564
Square	0.539653	0.347802	4.23371
Rectangular	0.556318	0.347361	4.36119
Triangle	0.282754	0.40213	3.55865

in Table 3. The correlations are within ±1.85% error margin with the numerical results. The correlations are valid for 500≤Re≤2000 and 0≤Φ≤0.05 vol.% Fe_3O_4/water nanofluid.

$$Nu = a \cdot \mathrm{Re}^{b} + c \cdot \varphi \quad (32)$$

CONCLUSION

In this study, flow and heat transfer characteristics of water and Fe_3O_4/water nanofluid flowing through channels of variable cross-section with the same hydraulic diameters were numerically investigated. Based on the data obtained from the study, the following conclusions have been reached.

- Nanoparticle dispersion into the base fluid enhances the heat transfer rate; on the other hand, it does not affect the friction factor drastically.
- Cylindrical cross-sectioned channel geometry offers best heat transfer performance with up to 77.6% convective heat transfer enhancement compared to triangle cross-sectioned channel geometry. Square cross-sectioned channel geometry up to 36.4%, and rectangular cross-sectioned channel geometry up to 40.1% enhancement compared to triangle cross-sectioned channel geometry for the same hydraulic diameter and same heat flux. Triangle cross-sectioned channel geometry shows worst heat transfer performance among all.
- Up to 3.67% convective heat transfer enhancement is achieved in cylindrical cross-sectioned channel geometry using nanofluid as working fluid compared to the distilled water. Square and rectangular cross-sectioned channel geometries offer up to 3.9% enhancement; whereas the triangle cross-sectioned channel geometry offers up to 4.12% enhancement using nanofluid as working fluid compared to the distilled water. The best convective heat transfer increment using nanofluid compared to distilled water is achieved in triangular geometry.
- Triangle cross-sectioned channel geometry has the highest PEC number, while the cylindrical has the lowest. This doesn't mean that its efficiency is highest. PEC shows that using nanofluid on triangle cross-sectioned channel geometry further increases Nusselt number, compared to the other channel geometries.
- Cylindrical cross-sectioned channel geometry is best at entropy generation, triangle cross-sectioned channel geometry is the worst among all. It is the result of heat accumulation at the edges of non-circular cross-sectioned channel geometries and higher wall temperatures are reached here.
- Lower Reynolds numbers has higher entropy generation rate than higher Reynolds numbers. This is related with the wall temperature.
- Higher volumetric nanoparticle concentration of nanofluids have lower entropy generation rate then lower volumetric nanoparticle concentration of nanofluids and base fluids.5 vol.% nanofluid offers 12.1% lower entropy generation rate, while 2 vol.% offers 5.5% lower, 1 vol.% offers 2.9% lower entropy generation compared to water.

ACKNOWLEDGEMENT

The authors would like to thank Scientific and Technological Research Council of Turkey (TUBİTAK, Project no: 217M978) and Karabük University, Scientific Research Project Foundation (KBÜBAP Project Number: KBÜBAP-18-DR-185) for providing financial support for this study.

NOMENCLATURE

A	Surface area of the cross-section duct (m^2)
C_p	Specific heat (kJ kg^{-1} K^{-1})
D_h	Hydraulic diameter (m)
h	Average convective heat transfer coefficient (W m^{-2} K^{-1})
k	Thermal conductivity (W m^{-1} K^{-1})
L	Channel length (m)
Nu	Nusselt number
Pr	Prandtl number
q''	Heat flux (W m^{-2})
Re	Reynolds number
T_b	Bulk temperature (K)
T_w	Wall temperature (K)
V	Average fluid velocity (m s^{-1})
x	Axial length (m)

Greek symbols

μ	Viscosity (Pa s)
φ	Volumetric nanoparticle concentration (%)
ρ	Density (kg m^{-3})

Subscripts

n_f	Nanofluid
b_f	Base fluid

n_p	Nanoparticle
w	Wall
in	Inlet
out	Outlet
f	Fluid

AUTHORSHIP CONTRIBUTIONS

Authors equally contributed to this work.

DATA AVAILABILITY STATEMENT

The authors confirm that the data that supports the findings of this study are available within the article. Raw data that support the finding of this study are available from the corresponding author, upon reasonable request.

CONFLICT OF INTEREST

The author declared no potential conflicts of interest with respect to the research, authorship, and/or publication of this article.

ETHICS

There are no ethical issues with the publication of this manuscript.

REFERENCES

[1] Choi SS, Eastman AA. Enhancing thermal conductivity of fluids with nanoparticles. o ASME International Mechanical Engineering Congress & Exposition, November 12-17,1995, San Francisco, CA. ASME Puplications FED; 1995. p. 99–105.

[2] Wong K V, De Leon O. Applications of Nanofluids: Current and Future. Adv Mech Eng 2010;2:519659. [CrossRef]

[3] Şenay G, Kaya M, Gedik E, Kayfeci M. Numerical investigation on turbulent convective heat transfer of nanofluid flow in a square cross-sectioned duct. Int J Numer Methods Heat Fluid Flow 2019 Jan 7. doi: 10.1108/HFF-06-2018-0260. [Epub ahead of print]. [CrossRef]

[4] Yiamsawas T, Mahian O, Dalkilic AS, Kaewnai S, Wongwises S. Experimental studies on the viscosity of TiO2 and Al2O3 nanoparticles suspended in a mixture of ethylene glycol and water for high temperature applications. Appl Energy 2013;111:40–45. [CrossRef]

[5] S Dalkilic A, Kayaci N, Celen A, Tabatabaei M, Yildiz O, Daungthongsuk W, et al. Forced convective heat transfer of nanofluids - a review of the recent literature. Curr Nanosci 2012;8:949–969. [CrossRef]

[6] Minea AA. Numerical simulation of nanoparticles concentration effect on forced convection in a tube with nanofluids. Heat Transf Eng 2015;36:1144–1153. [CrossRef]

[7] Arslan K, Ekiciler R. Effects of sio2/water nanofluid flow in a square cross-sectioned curved duct.Eur J Eng Nat Sci 2019;3:101–109.

[8] Ting HH, Hou SS. Numerical study of laminar flow forced convection of water-al 2 o 3 nanofluids under constant wall temperature condition. Math Probl Eng 2015;2015:180841. [CrossRef]

[9] Heris SZ, Nassan TH, Noie SH, Sardarabadi H, Sardarabadi M. Laminar convective heat transfer of Al2O3/water nanofluid through square cross-sectional duct. Int J Heat Fluid Flow 2013;44:375–382. [CrossRef]

[10] Heris SZ, Kazemi-Beydokhti A, Noie SH, Rezvan S. Numerical Study on Convective Heat Transfer of AL 2 O 3 /Water, CuO/Water and Cu/Water Nanofluids through Square Cross-Section Duct in Laminar Flow. Eng Appl Comput Fluid Mech 2012;6:1–14. [CrossRef]

[11] Yin Z, Bao F, Tu C, Hua Y, Tian R. Numerical and experimental studies of heat and flow characteristics in a laminar pipe flow of nanofluid. J Exp Nanosci 2018;13:82–94. [CrossRef]

[12] Purohit N, Purohit VA, Purohit K. Assessment of nanofluids for laminar convective heat transfer: a numerical study. Eng Sci Technol an Int J 2016;19:574–586. [CrossRef]

[13] Li Q, Xuan Y. Convective heat transfer and flow characteristics of Cu-water nanofluid. Sci China, Ser E Technol Sci 2002;45:408–416.

[14] Wen D, Ding Y. Experimental investigation into convective heat transfer of nanofluids at the entrance region under laminar flow conditions. Int J Heat Mass Transf 2004;47:5181–5188. [CrossRef]

[15] Chen H, Yang W, He Y, Ding Y, Zhang L, Tan C, et al. Heat transfer and flow behaviour of aqueous suspensions of titanate nanotubes (nanofluids). Powder Technol 2008;183:63–72. [CrossRef]

[16] Anoop KB, Sundararajan T, Das SK. Effect of particle size on the convective heat transfer in nanofluid in the developing region. Int J Heat Mass Transf 2009;52:2189–2195. [CrossRef]

[17] Davarnejad R, Barati S, Kooshki M. CFD simulation of the effect of particle size on the nanofluids convective heat transfer in the developed region in a circular tube. Springerplus. 2013 Apr 30;2:192. [CrossRef]

[18] Abareshi M, Goharshadi EK, Zebarjad SM, Fadafan HK, Youssefi A. Fabrication, characterization and measurement of thermal conductivity of Fe3O4 nanofluids. J Magn Magn Mater 2010;322:3895–3901. [CrossRef]

[19] Turgut A, Tavman I, Chirtoc M, Schuchmann HP, Sauter C, Tavman S. Thermal Conductivity and Viscosity Measurements of Water-Based TiO2

Nanofluids. Int J Thermophys 2009;30:1213–1226. [CrossRef]
[20] Fadhil AM, Khalil WH, Al-damook A. The hydraulic-thermal performance of miniature compact heat sinks using SiO2-water nanofluids. Heat Transf Res 2019;48:3101–3114. [CrossRef]
[21] Kaya H, Ekiciler R, Arslan K. CFD analysis of laminar forced convective heat transfer for tio2/water nanofluid in a semi-circular cross-sectioned micro-channel. J Therm Eng 2019;5:123–137. [CrossRef]
[22] Uysal C, Arslan K, Kurt H. Laminar forced convection and entropy generation of ZnO-ethylene glycol nanofluid flow through square microchannel with using two-phase Eulerian-Eulerian model. J Appl Fluid Mech 2019;12:1–10. [CrossRef]
[23] Uysal C, Gedik E, Chamkha AJ. A Numerical analysis of laminar forced convection and entropy generation of a diamond-Fe3O4/water hybrid nanofluid in a rectangular minichannel. j appl fluid mech 2019;12:391–402. [crossref]
[24] Li Z, Sheikholeslami M, Jafaryar M, Shafee A, Chamkha A. Investigation of nanofluid entropy generation in a heat exchanger with helical twisted tapes. J Mol Liq 2018;266:797–805. [CrossRef]
[25] Incropera FP, DeWitt DP, Bergman TL, Lavine AS. Fundamentals of Heat and Mass Transfer. 6th ed. Hoboken, New Jersey, ABD. 2007.
[26] Shah RK, London AL. Laminar Flow Forced Convection in Ducts: A Source Book for Compact Heat Exchanger Analytical Data.Cambridge, Massachusetts,USA. Academic Press;1978.
[27] Gnielinski V. G1 Heat Transfer in Pipe Flow. In: VDI V, editors. VDI Heat Atlas. VDI-Buch. Berlin:Springer; 2010. [CrossRef]
[28] Churchill SW, Ozoe H. Correlations for Laminar Forced Convection with Uniform Heating in Flow over a Plate and in Developing and Fully Developed Flow in a Tube. J Heat Transfer 1973;95:78–84. [CrossRef]
[29] Mills AF. Basic heat and mass transfer. 2nd ed. New Jersey: Prentice hall; 1999.
[30] Maxwell JC. A treatise on electricity and magnetism. vol. 1. Clarendon press. ABD:Boca Raton, Florida; 1873.
[31] Lide DR. Crc handbook of chemistry and physics: a ready-reference book of chemical and physical data. CRC press. ABD:Boca Raton, Florida; 1995.
[32] Yang C, Wu X, Zheng Y, Qiu T. Heat transfer performance assessment of hybrid nanofluids in a parallel channel under identical pumping power. Chem Eng Sci 2017;168:67–77. [CrossRef]
[33] Dibaei M, Kargarsharifabad H. New Achievements in Fe3O4 Nanofluid Fully Developed Forced Convection Heat Transfer under the Effect of a Magnetic Field: An Experimental Study. J Heat Mass Transf Res 2016;4:1–12.
[34] A. Bejan. Entropy Generation Minimization: The new thermodynamics of finite-size devices and finite-time processes. Boca Raton, NY: CRC Press; 1996. [CrossRef]
[35] Cengel, YA. and Boles M. Thermodynamics: An Engineering Approach. 8th ed. New York:McGraw-Hill Education; 2014.
[36] Minea AA. Challenges in hybrid nanofluids behavior in turbulent flow: Recent research and numerical comparison. Renew Sustain Energy Rev 2017;71:426–434. [CrossRef]
[37] Jiji LM. Heat convection. Berlin:Springer; 2006.
[38] Morrison FA. Data Correlation for Drag Coefficient for Sphere. Dep Chem Eng Michigan Technol Univ Houghton, MI 2013;49931.